

Polymer Chemistry

Accepted Manuscript



This is an *Accepted Manuscript*, which has been through the Royal Society of Chemistry peer review process and has been accepted for publication.

Accepted Manuscripts are published online shortly after acceptance, before technical editing, formatting and proof reading. Using this free service, authors can make their results available to the community, in citable form, before we publish the edited article. We will replace this *Accepted Manuscript* with the edited and formatted *Advance Article* as soon as it is available.

You can find more information about *Accepted Manuscripts* in the [Information for Authors](#).

Please note that technical editing may introduce minor changes to the text and/or graphics, which may alter content. The journal's standard [Terms & Conditions](#) and the [Ethical guidelines](#) still apply. In no event shall the Royal Society of Chemistry be held responsible for any errors or omissions in this *Accepted Manuscript* or any consequences arising from the use of any information it contains.

ARTICLE

Pyrrolophthalazine Dione (PPD)-based Donor-Acceptor Polymers as High Performance Electrochromic Materials

Cite this: DOI: 10.1039/x0xx00000x

Received 00th January 2014,
Accepted 00th January 2014

DOI: 10.1039/x0xx00000x

www.rsc.org/Qun Ye,^{+,a} Wei Teng Neo,^{+,a,b} Tingting Lin,^a Jing Song,^a Hong Yan,^a Hui Zhou,^a
Kwok Wei Shah,^a Soo Jin Chua,^{a,c} and Jianwei Xu^{a,d,*}

A novel pyrrolophthalazine dione (PPD) acceptor was sophisticatedly designed and synthesized via inverse electron demand Diels-Alder reaction, followed by aromatization with N-bromosuccinimide. The PPD moiety was incorporated into donor-acceptor type conjugated polymers through Stille coupling polymerization to yield a series of polymers **P1-P3** with different linking groups, namely, thiophene, thieno[3,2-*b*]thiophene and bithiophene. The polymers reveal excellent solubility in common organic solvents. Due to their low band gaps of around 1.72-1.78 eV, the polymers show broad absorption that covers most of the visible region. All the polymers reveal electrochromism, switching between dark blue and transmissive sky blue states. In particular, **P2** exhibits exceptional electrochromic properties with high optical contrasts of up to 34 and 71 % in the visible and NIR regions, high coloration efficiencies of 471 and 651 cm²/C respectively, as well as reasonable switching speeds and good long-term stability.

Introduction

Polymer-based electrochromic materials¹⁻³ are promising candidates for the next-generation color-changing technologies, owing to their numerous advantages. Compared to their inorganic counterparts and conventional liquid crystal materials, conjugated polymers possess properties such as color-tunability,⁴⁻⁷ low cost, lightweight,⁸ thin-film flexibility,⁹ low power consumption¹⁰ and wide-viewing angles.¹¹

Electrochromic conjugated polymers can be largely categorized into two major groups based on the nature of the constituting monomer(s) – all-donor and donor-acceptor (DA) type. The former is made up of solely electron-rich units, and popular examples include homopolymers of ethylenedioxythiophene (EDOT),¹² propylenedioxythiophene (ProDOT)¹³⁻¹⁵ and dialkoxythiophene (DalkOT).¹⁶⁻¹⁸ In the latter, the polymer chain consists of alternating electron-donating and electron-accepting groups.¹⁹ Between the two approaches, the DA approach has gained more popularity within the scientific community. One of the most fundamental functions of the DA approach is to create low band-gap polymers,²⁰ through the tuning of the highest occupied molecular orbital (HOMO) and the lowest unoccupied molecular orbital (LUMO) energy levels. Moreover, dual absorption peaks⁴ characteristic of DA polymers have also been ingeniously utilized by researchers for

color-tuning, especially for the creation of neutral-state green²¹⁻²⁶ and black^{13, 27-30} polymers. Besides, it is well documented by many groups that DA type conjugated polymers give high electrochromic performance in terms of optical contrasts, switching speeds, coloration efficiencies and stabilities. Such favourable parameters can largely be attributed to the strong intramolecular interactions for efficient charge transport and low-lying HOMO levels for ambient stability.³¹

Much attention has been focused on pushing electrochromic polymers towards a state of commercial viability.³² As such, an area of extensive research has been on the exploration and development of novel materials and building blocks. As thiophene-based EDOT and ProDOT have established themselves as efficient donor building blocks, much emphasis has been placed on the investigation of newer and more effective acceptor units. Extensive investigations have been carried out on benzothiadiazole^{31, 33-35} and benzotriazole,³⁶⁻³⁸ as well as quinoxaline^{39, 40} and imidazole^{41, 42}, and considerable success has been attained. We are particularly interested in the design and development of new electron-deficient acceptor monomers for DA type conjugated polymers. Recently we have discovered that inverse electron demand Diels-Alder reaction between tetrazine and dienophiles can be adopted as a reliable methodology to prepare pyridazine based acceptors.⁴³ By

extending the chemical strategy that we have developed, herein, we would like to report a novel acceptor moiety 7-alkyl-6*H*-pyrrolo[3,4-*g*]phthalazine-6,8(7*H*)-dione (PPD) and its application as electrochromic materials. This acceptor monomer is designed to have strong electron deficiency owing to the presence of electron withdrawing imide and pyridazine moieties. Moreover, as the imide group is open to easy side chain engineering, the prepared polymers are thus envisaged to have sufficient solubility to make solution-based processing techniques viable. To prove this, a series of PPD-containing conjugated polymers with electron-donating thiophene based monomers and ProDOT moieties have been synthesized and characterized. The potential of PPD as an effective building block for electrochromic conjugated polymers has also been demonstrated.

Experimental

Materials

All reagents and starting materials were obtained from commercial sources and used without further purification. ITO-coated glass substrates (15 Ω/sq, 35×30×1.1mm) were purchased from Xinyan Technology Ltd.

Monomer synthesis

1,4-Bis(5-bromothiophen-2-yl)-7-(2-octyldodecyl)-5,5a,8a,9-tetrahydro-6*H*-pyrrolo[3,4-*g*]phthalazine-6,8(7*H*)-dione (2). To a dry round bottom flask was added 3,6-bis(5-bromothiophen-2-yl)-1,2,4,5-tetrazine (3g, 7.43mmol), 2-(2-octyldodecyl)-3a,4,7,7a-tetrahydro-1*H*-isoindole-1,3(2*H*)-dione (3.19g, 7.43mmol) and diphenyl ether (20ml). The mixture was purged with argon for 15 min and then heated to 160 °C for 16h. After cooling to room temperature, the mixture was directly subjected to silica gel column chromatography. Hexane was first used to flush away the diphenyl ether. The target compound was then collected as yellow oil using mixture solvent (Hex:CHCl₃ =1:1) then CHCl₃ as eluent (3.40g, 57%). Due to the oily nature of the product, it was contaminated by ca. 5% of starting material. The crude product was used for the next step without further purification. HR-APCI-MS: *m/z* = 804.1870, calculated exact mass: 804.1862, error: 0.9 ppm.

1,4-Bis(5-bromothiophen-2-yl)-7-(2-octyldodecyl)-6*H*-pyrrolo[3,4-*g*]phthalazine-6,8(7*H*)-dione (3). To a dry round bottom flask was added 1,4-bis(5-bromothiophen-2-yl)-7-(2-octyldodecyl)-5,5a,8a,9-tetrahydro-6*H*-pyrrolo[3,4-*g*]phthalazine-6,8(7*H*)-dione (1g, 1.25 mmol), NBS (2.2 equiv. 490mg, 2.75mmol), benzoyl peroxide (0.1 equiv, 0.125mmol, 30mg) and dichloroethane (20ml). The mixture was purged with argon for 15 min and then heated to 120 °C for 2 days. After cooling to room temperature, the solvent was removed by rotary evaporation. The residue was directly subjected to silica gel column chromatography to afford the target molecule as a yellow powder (720mg, 72%). ¹H NMR (400 MHz, CDCl₃): δ ppm = 8.93 (s, 2H), 7.52-7.51 (d, 2H, *J* = 4 Hz), 7.28-7.27 (d, 2H, *J* = 4 Hz), 3.71-3.69 (d, 2H, *J* = 7.2 Hz), 1.94 (m, 1H), 1.29-

1.23 (m, 32H), 0.88-0.84 (m, 6H). ¹³C NMR (100MHz, CDCl₃): δ ppm = 166.84, 152.67, 140.05, 134.21, 131.63, 131.41, 127.56, 122.31, 119.06, 43.60, 37.41, 32.28, 31.89, 30.33, 30.02, 29.69, 26.66, 23.06, 14.50. HR-EI-MS: *m/z* = 801.1470, calculated exact mass: 801.1456, error: 1.81 ppm.

1,4-Bis(5-(3,3-bis((dodecyloxy)methyl)-3,4-dihydro-2*H*-thieno[3,4-*b*][1,4]dioxepin-6-yl)thiophene-2-yl)-7-(2-octyldodecyl)-6*H*-pyrrolo[3,4-*g*]phthalazine-6,8(7*H*)-dione (4). To a dry round bottom flask was added (3,3-bis((dodecyloxy)methyl)-3,4-dihydro-2*H*-thieno[3,4-*b*][1,4]dioxepin-6-yl)trimethylstannane (2 g, 50% purity), 1,4-bis(5-bromothiophen-2-yl)-7-(2-octyldodecyl)-6*H*-pyrrolo[3,4-*g*]phthalazine-6,8(7*H*)-dione (370mg, 0.47 mmol), Pd(PPh₃)₄ (0.1 equiv, 0.047 mmol, 54 mg) and dry toluene (15ml). The mixture was degassed by purging with argon and then heated to 110 °C for 16h. After cooling to room temperature, the solvent was removed by rotary evaporation. The collected residue was dissolved in minimum amount of chloroform and directly subjected to silica gel column chromatography. The target compound was then collected as red waxy solid using mixture solvent (Hex:CHCl₃ =1:1) (510mg, 62%). The target compound was found to be unstable at ambient condition. It was stored in the fridge after preparation. ¹H NMR (400 MHz, CDCl₃): δ ppm = 9.00 (s, 2H), 7.68 (d, 2H, *J* = 3.6 Hz), 7.38-7.37 (d, 2H, *J* = 4 Hz), 6.45 (s, 2H), 4.22 (s, 4H), 4.10 (s, 4H), 3.71-3.69 (d, 2H, *J* = 7.2 Hz), 3.55 (m, 8H), 3.44-3.41 (m, 8H), 1.94 (m, 1H), 1.68 (m, 4H), 1.56-1.54 (m, 8H), 1.30-1.24 (m, 100H), 0.88-0.85 (m, 18H). ¹³C NMR (100MHz, CDCl₃): δ ppm = 167.06, 152.76, 150.41, 147.06, 141.15, 136.18, 134.00, 131.31, 127.99, 123.98, 122.81, 116.59, 103.85, 74.41, 72.20, 70.00, 48.25, 43.53, 37.41, 32.33, 31.89, 30.36, 30.08, 29.97, 29.77, 26.58, 23.09, 14.52. HR-APCI-MS: *m/z* = 1744.1423, calculated exact mass: 1744.1411, error: 0.67 ppm.

1,4-Bis(5-(8-bromo-3,3-bis((dodecyloxy)methyl)-3,4-dihydro-2*H*-thieno[3,4-*b*][1,4]dioxepin-6-yl)-7-(2-octyldodecyl)-6*H*-pyrrolo[3,4-*g*]phthalazine-6,8(7*H*)-dione (5). To a dry round bottom flask was added 1,4-Bis(5-(3,3-bis((dodecyloxy)methyl)-3,4-dihydro-2*H*-thieno[3,4-*b*][1,4]dioxepin-6-yl)thiophene-2-yl)-7-(2-octyldodecyl)-6*H*-pyrrolo[3,4-*g*]phthalazine-6,8(7*H*)-dione (1 g, 0.573 mmol), NBS (2.2 equiv., 1.26mmol, 225mg) and chloroform (10ml). The mixture was stirred at room temperature overnight. The solvent was removed by rotary evaporation and the residue was directly subjected to silica gel chromatography using hexane: chloroform (1:1) to get the target product as a red waxy solid (0.92g, 85%). ¹H NMR (400 MHz, CDCl₃): δ ppm = 8.98 (s, 2H), 7.66-7.65 (d, *J* = 4 Hz, 2H), 7.30-7.29 (d, *J* = 4 Hz, 2H), 4.22 (s, 4H), 4.17 (s, 4H), 3.71-3.69 (d, *J* = 7.2 Hz, 2H), 3.55 (s, 8H), 3.44-3.41 (t, *J* = 6.4 Hz, 8H), 1.91 (m, 1H), 1.55-1.24 (m, 112H), 0.88-0.85 (m, 18H). ¹³C NMR (100MHz, CDCl₃): δ ppm = 167.02, 152.76, 148.45, 145.93, 139.98, 133.99, 131.14, 127.78, 124.09, 123.11, 122.72, 116.27, 92.92, 74.67, 72.19, 69.90, 48.31, 43.53, 37.43, 32.31, 31.89, 30.35, 30.09, 26.60, 23.11, 14.54. HR-APCI-MS: *m/z* = 1901.9589, calculated exact mass: 1901.9568, error: 1.17 ppm.

Polymer synthesis

General procedure for Stille cross-coupling polymerization. 1,4-Bis(5-(8-bromo-3,3-bis((dodecyloxy)methyl)-3,4-dihydro-2*H*-thieno[3,4-*b*][1,4]dioxepin-6-yl)-7-(2-octyldodecyl)-6*H*-pyrrolo[3,4-*g*]-phthalazine-6,8(7*H*)-dione (300mg, 0.158 mmol) and bis(trimethylstannyl) compounds (0.158 mmol) were dissolved in 10 ml of toluene. The mixture was stirred and purged with argon for about 15 min, and then Pd(PPh₃)₄ (6% equiv., 0.00948mmol, 11mg) was added. The flask was purged with argon for another 15 min before the mixture was heated to 110 °C for 2 days. Excess solvent was removed under reduced pressure and the polymer was precipitated with methanol. The suspension was filtered to give the crude product, which was then purified by Soxhlet extraction with acetone and chloroform. The chloroform fraction was evaporated to dryness to afford the target polymer materials.

Polymer P1. Yield 74%. ¹H NMR (main signals) (CDCl₃): δ 9.09 (br), 7.92 (br), 4.31 (br, m), 3.72-3.45 (br, m), 1.68-1.58 (br, m), 1.24 (m), 0.87 (m).

Polymer P2. Yield 72%. ¹H NMR (main signals) (CDCl₃): δ 8.99 (br), 7.65 (br), 4.33 (br), 3.62-3.48 (br, m), 1.24 (br, m), 0.86 (br, m).

Polymer P3. Yield 55%. ¹H NMR (main signals) (CDCl₃): δ 9.08 (br), 7.82 (br), 6.97 (br), 4.31(br), 3.70-3.48 (br, m), 1.79-1.68 (br), 1.24 (br), 0.86(br).

Electrochromic device fabrication

Prior to use, ITO/glass substrates were cleaned by successive ultrasonication in acetone, isopropyl alcohol and distilled water, and blown dry with N₂. Polymer solutions of **P1-P3** were prepared at a concentration of 15 mg/mL in 6:4 (v/v) chloroform:chlorobenzene mixed solvent. Warm polymer solution (50 °C) was filtered and spin-coated onto the heated ITO substrates (50 °C) at 1200 rpm for 60 s to yield film thickness of around 100 nm. For drop-cast films, the polymer solutions are dispensed, spread onto the ITO substrates and left to dry. Film thickness of approximately 150-200 nm was obtained. Excessive polymer edges were removed by swabbing with chloroform using a cotton bud to obtain an active area of 2×2 cm². On a second piece of ITO substrate, an area of 2×2 cm² was blocked out using parafilm. The total thickness of the parafilm spacer and barrier was kept constant at 0.01". 250 μL of the gel electrolyte (0.512 g of lithium perchlorate and 2.8 g of poly(methyl methacrylate) (MW = 120,000 g/mol) in 6.65 ml of propylene carbonate and 28 ml of dry acetonitrile) was pipetted within the 2×2 cm² area. The device was fabricated by assembling the two ITO/glass substrates together with the polymer film and gel electrolyte in contact.

Instrumentation

¹H and ¹³C NMR spectra were recorded using Avance 400 MHz Bruker spectrometer in CDCl₃. All chemical shifts are quoted in ppm, relative to tetramethylsilane, using the residual solvent peak as a reference standard. Molecular weights were determined using an Alliance Waters model 2690 Gel Permeation Chromatography system calibrated with PMMA as

the standard and THF as the eluent. HR-EI-MS was carried out on Finnigan TSQ 7000 triple stage quadrupole mass spectrometer. HR-APCI-MS was carried out on AmaZon X with Dionex Ultimate 3000 RSLC system and Kd Science Syringe pump infusion system. A Shimadzu UV-3600 UV-vis-NIR spectrophotometer was used to record all absorption spectra. Cyclic voltammetry was carried out using an Autolab PGSTAT128N potentiostat. Measurements were done in a MBraun LABmaster 130 glove box, in a three-electrode cell configuration with polymer-coated glassy carbon, Pt and Ag wires as the working, counter and pseudo-reference electrodes respectively, at a scan rate of 50 mV/s. A 0.1 M LiClO₄/ACN electrolyte/solvent couple was used. The pseudo-reference electrode was calibrated against the ferrocene/ferrocenium redox couple. All electrochromic studies were performed *in-situ*, using both the potentiostat and spectrophotometer. AFM images were obtained under tapping mode, using Bruker Dimension IconTM atomic force microscope.

Results and discussion

Synthesis and characterization

The synthesis of PPD embedded EC polymers **P1-P3** is outlined in **Scheme 1**. Starting from compound **1**, inverse electron demand Diels-Alder reaction between **1** and 2-(2-octyldodecyl)-4,7-dihydro-1*H*-isoindole-1,3(2*H*)-dione occurred smoothly at 160 °C in diphenyl ether to afford the adduct product **2** in 57% yield. Aromatization of **2** with *N*-bromosuccinimide in refluxing 1,2-dichloroethane directly afforded the aromatized species **3** in 72% yield. This is rather unexpected as generally a dibrominated intermediate is generated and aromatization is assisted with treatment of base.⁴⁴ This could be rationalized by heat assisted dehydrobromination which happened after the radical bromination. The following Stille coupling on **3** introduced two alkylated thieno[3,4-*b*][1,4]dioxepine units onto the backbone to afford compound **4** in 62% yield. The purposes to introduce these two alkylated thieno[3,4-*b*][1,4]dioxepine units are to improve the solubility and stability of the final polymers. Bromination of **4** under mild condition (NBS, CHCl₃, rt.) gave the dibrominated monomer **5** in 85% yield. The dibrominated monomer **5** was then subjected to Stille coupling polymerization with 2,5-bis(trimethylstannyl)thiophene, 2,5-bis(trimethylstannyl)thieno[3,2-*b*]thiophene and 5,5'-bis(trimethylstannyl)-2,2'-bithiophene to afford **P1-P3**, respectively in 55-75% yield. All three polymers exhibited comparable M_n of around 20,000 Da and good thermal stability with T_d > 270 °C (Table 1). No observable phase transition was observed for these three polymers due to the presence of branched alkyl chains.⁴⁵

Optical properties

The normalized UV-vis absorption spectra of the polymers in chlorobenzene and as thin films are shown in Fig. 1a and the

spectroscopic data are summarized in Table 2. All the polymers reveal broad absorptions that cover the 400–700 nm range, with noticeable dual absorptions characteristic of donor-acceptor type polymers. Going from the solution to film states, all the polymers exhibit spectra broadening with bathochromic shifts in the absorption maxima, suggesting the presence of aggregation in the solid state. From the absorption onsets of the polymer films, the optical band gaps of **P1–P3** were approximated to be 1.72, 1.78 and 1.72 eV respectively. The identity of the linkers used here, i.e., thiophene, thieno[3,2-*b*]thiophene and bithiophene, does not significantly influence the optical properties of the final polymers. This can be rationalized by the very similar frontier orbital distributions for three polymers as revealed by TD-DFT calculations (*vide infra*).

Electrochemical properties

Cyclic voltammetry was employed to investigate the redox behaviour and frontier orbital energy levels of the polymers. The cyclic voltammograms of the polymer thin films are shown in Fig. 1b and the electrochemical data are tabulated in Table 2. All the polymers exhibit quasi-reversible redox properties, with **P2** revealing the highest reversibility and electroactivity. Based on the oxidation onset potentials, the HOMO energy levels of **P1–P3** were very close to one another and estimated to -5.27, -5.29 and -5.28 eV respectively. With deep HOMO positions, the polymers are expected to display good ambient stability. Upon n-doping at negative applied potentials no distinct redox peaks were observed and hence the LUMO energy levels could only be approximated from the optical band gaps all three polymers **P1–P3** exhibited similar LUMO energy levels at -3.51 ~ -3.56 eV.

Computational calculations

To better understand the minimum-energy conformation and frontier molecular orbitals distribution of the polymers, time-dependent density functional theory (TD-DFT) calculations at B3LYP/6-31G(d) theory level was carried out for the simplified monomeric model compounds of **M1–M3** (Fig. 2). All the substitution -R groups are replaced with methyl groups for simplicity. In general, model compounds **M1–M3** display relatively high molecular planarity. The torsional angle between the PPD acceptor and neighbouring thiophene units is ca. 30°, hence rendering good conjugation between donor and acceptor moieties along the π -backbone (see supporting information). It is observed that for all the model compounds, the HOMO is well-delocalized over the entire π -backbone with a typical alternating phase changing pattern which is routinely observed for conjugated polymers.^{46–48} On the other hand, the LUMO is mainly localized on the PPD acceptor moiety and slightly extended to the neighbouring thiophene units. The linker moieties are found to have minor influence over the whole electron distribution on the frontier orbitals.

Electrochromic properties and performance

The spectroelectrochemical behaviour of **P1–P3** were analysed in fabricated electrochromic devices (ECDs) to closely represent their functional capabilities in real-life applications. Common liquid electrolytes employed for electrochromic thin film studies may be unpractical and infeasible.⁴⁹ Due to the limited film-forming ability of **P1** and **P3**, polymer thin films were obtained from drop-casting. For **P2**, spin-coating was employed and a drop-casted device was also fabricated for comparison. The spectroelectrochemical graphs for polymers **P1–P3** are illustrated in Figs. 3, S1 and S2. In general, all three polymers reveal electrochromism, switching between a dark blue state and a transmissive sky blue hue (Fig. 4). As observed for **P2**, spectra differences between the spin-coated and drop-cast devices are apparent. For the spin-coated device, the absorption in the visible region depletes upon gradual oxidation, with concomitant formation of the polaron and bipolaron bands in the NIR region. The polaron absorption occurs at around 800 nm and peaks at 1.5 V. Upon further bias, the polarons are fully converted into the bipolarons, as evident from the increase in absorption intensity at 1220 nm. Distinct isosbestic points at 660 and 884 nm confirm the presence of the interconverting species.⁵⁰ On the other hand, the drop-cast device reveals a reduced propensity towards oxidation, as evident from the higher bias required and smaller decrease in intensity of the visible absorption. Moreover, only one isosbestic point was observed. This proves that the polymer is saturated with polaronic states that are unable to further convert to bipolarons even at increased bias. The reduction in electroactivity of the drop-cast device compared to the spin-coated device is most likely due to the non-uniform, compact and thicker surface which inhibits the movement of charges and counter ions.

The electrochromic properties of **P2** (spin-coated), **P1** and **P3** (drop-cast) devices were characterized using *in-situ* square-wave potential step absorptiometry. Transmittance changes of the polymers at λ_{max} and 1400 nm were measured while the devices were subjected to repeated redox cycles between +1.6 and -1.6 V at a residence time of 30 s. The electrochromic response data is shown in Figs. 5, S3 and S4, and summarized in Table 3. For **P2**, the optical contrasts are remarkable at 34 and 71 % in the visible and NIR regions respectively. Switching times were subsequently calculated as the time required to reach 95 % of the full switch. An asymmetry in the bleaching and coloration times is observed, with switching speeds in the range of 1.8 to 23 s. For **P1** and **P3**, despite the lack of electroactivity in the drop-cast films, respectable contrasts of up to 62 % and switching times of 4 s were attained. With better device optimization, enhanced electrochromic performance can be expected for all the polymers. Moreover, high coloration efficiencies (CE) were measured for **P1–P3** devices. In particular, **P2** reveals values of 471 and 651 cm²/C in the visible and NIR regions respectively,

which are drastically higher than the standard blue-to-transmissive switching PEDOT (183 cm²/C).⁵¹

Stability studies for **P2** device was carried out by monitoring the optical contrast as a function of number of cycles. Potentials of +1.6 and -1.6 V were applied with a residence time of 15 s. The polymer exhibits good switching stability, and an illustration of 10 repeated cycles is given in Fig. 6. After reaching a state of equilibrium, the device was further cycled for 1000 cycles. Over the entire duration, approximately 75 % of the optical contrast was retained (Fig. S5).

Thin film morphology

The surface morphologies of **P2** spin-coated and drop-cast films were also probed using atomic force microscopy over a 5×5 μm area and the height images are shown in Fig. 7. The spin-coated film shows a more uniform and homogenous surface with a mean surface roughness of 1.94 nm. In contrast, the drop-cast film reveals larger polymer aggregates of different sizes. Moreover, the formation of ridges gives rise to an increased surface roughness of 2.69 nm. Due to the clustering of the polymer, exposed surface area is reduced and movement of the counter ions to oxidized sites of the polymer will be hindered during redox switching. This supports the observation of the reduced electroactivity of the drop-cast device. Also, this reinforces the notion that the film morphology plays an important role in the performance of electrochromic devices.^{52, 53}

Conclusions

A series of donor-acceptor type conjugated polymers was synthesized, by utilizing a novel pyrrolophthalazine dione (PPD) acceptor monomer. The polymers are dark blue in their neutral states, and turn transmissive sky blue upon oxidation. The PPD-embedded polymers reveal exceptional electrochromic properties such as high optical contrasts and coloration efficiencies, as well as respectable switching speeds and redox stability. As such, the PPD unit presents itself as a promising building block for conjugated polymers, in particular for electrochromic applications. Moreover, the PPD monomer would serve as an efficient acceptor moiety for other D-A type polymeric organic materials⁵⁴ such as field-effect transistors and organic photovoltaic solar cell materials. The viabilities of these approaches are currently under investigation in our lab.

Acknowledgements

This research was supported by Agency for Science, Technology and Research (A*STAR) and Ministry of National Development (MND) Green Building Joint Grant (No. 1321760011). This work was also supported by the A*STAR Computational Resource Centre through the use of its high performance computing facilities.

Notes and references

- ^a Institute of Materials Research and Engineering, A*STAR, 3 Research Link, Singapore 117602.
- ^b NUS Graduate School for Integrative Sciences and Engineering, National University of Singapore, 28 Medical Drive, Singapore 117456.
- ^c Department of Electrical and Computer Engineering, National University of Singapore, 4 Engineering Drive 3, Singapore 117583
- ^d Department of Chemistry, National University of Singapore, 3 Science Drive 3, Singapore 117543
- [†] These two authors contribute equally to this work.
- H.-J. Yen and G.-S. Liou, *Polymer Chemistry*, 2012, **3**, 255-264.
 - G. Sonmez, *Chemical Communications*, 2005, 5251-5259.
 - V. K. Thakur, G. Ding, J. Ma, P. S. Lee and X. Lu, *Advanced Materials*, 2012, **24**, 4071-4096.
 - P. M. Beaujuge, C. M. Amb and J. R. Reynolds, *Accounts of Chemical Research*, 2010, **43**, 1396-1407.
 - P. M. Beaujuge and J. R. Reynolds, *Chemical Reviews*, 2010, **110**, 268-320.
 - L. Beverina, G. A. Pagani and M. Sassi, *Chemical Communications*, 2014, **50**, 5413-5430.
 - J. Hou, M.-H. Park, S. Zhang, Y. Yao, L.-M. Chen, J.-H. Li and Y. Yang, *Macromolecules*, 2008, **41**, 6012-6018.
 - T. A. Skotheim and J. Reynolds, *Conjugated Polymers: Processing and Applications*, Taylor & Francis, 2006.
 - W. Knoll and R. C. Advincula, *Functional Polymer Films*, Wiley, 2013.
 - I. F. Perepichka and D. F. Perepichka, *Handbook of Thiophene-Based Materials: Applications in Organic Electronics and Photonics, 2 Volume Set*, Wiley, 2009.
 - P. R. Somani and S. Radhakrishnan, *Materials Chemistry and Physics*, 2003, **77**, 117-133.
 - J. C. Gustafsson-Carlberg, O. Inganäs, M. R. Andersson, C. Booth, A. Azens and C. G. Granqvist, *Electrochimica Acta*, 1995, **40**, 2233-2235.
 - P. M. Beaujuge, S. Ellinger and J. R. Reynolds, *Nat Mater*, 2008, **7**, 795-799.
 - B. D. Reeves, C. R. G. Grenier, A. A. Argun, A. Cirpan, T. D. McCarley and J. R. Reynolds, *Macromolecules*, 2004, **37**, 7559-7569.
 - C. L. Gaupp, D. M. Welsh and J. R. Reynolds, *Macromolecular Rapid Communications*, 2002, **23**, 885-889.
 - F. Garnier, G. Tourillon, M. Gizard and J. C. Dubois, *Journal of Electroanalytical Chemistry and Interfacial Electrochemistry*, 1983, **148**, 299-303.
 - C. Arbizzani, A. Bongini, M. Mastragostino, A. Zanelli, G. Barbarella and M. Zambianchi, *Advanced Materials*, 1995, **7**, 571-574.
 - M. Mastragostino, C. Arbizzani, A. Bongini, G. Barbarella and M. Zambianchi, *Electrochimica Acta*, 1993, **38**, 135-140.
 - E. E. Havinga, W. ten Hoeve and H. Wynberg, *Polymer Bulletin*, 1992, **29**, 119-126.
 - Y.-C. Hung, C.-Y. Chao, C.-A. Dai, W.-F. Su and S.-T. Lin, *The Journal of Physical Chemistry B*, 2012, **117**, 690-696.
 - G. E. Gunbas, A. Durmus and L. Toppare, *Advanced Materials*, 2008, **20**, 691-695.

22. P. M. Beaujuge, S. V. Vasilyeva, D. Y. Liu, S. Ellinger, T. D. McCarley and J. R. Reynolds, *Chemistry of Materials*, 2012, **24**, 255-268.
23. P. M. Beaujuge, S. Ellinger and J. R. Reynolds, *Advanced Materials*, 2008, **20**, 2772-2776.
24. S. Hellström, T. Cai, O. Inganäs and M. R. Andersson, *Electrochimica Acta*, 2011, **56**, 3454-3459.
25. G. Sonmez, C. K. F. Shen, Y. Rubin and F. Wudl, *Angewandte Chemie International Edition*, 2004, **43**, 1498-1502.
26. G. Sonmez, H. B. Sonmez, C. K. F. Shen, R. W. Jost, Y. Rubin and F. Wudl, *Macromolecules*, 2005, **38**, 669-675.
27. M. İçli, M. Pamuk, F. Algi, A. M. Önal and A. Cihaner, *Organic Electronics*, 2010, **11**, 1255-1260.
28. F. C. Krebs, *Nat Mater*, 2008, **7**, 766-767.
29. P. Shi, C. M. Amb, E. P. Knott, E. J. Thompson, D. Y. Liu, J. Mei, A. L. Dyer and J. R. Reynolds, *Advanced Materials*, 2010, **22**, 4949-4953.
30. S. V. Vasilyeva, P. M. Beaujuge, S. Wang, J. E. Babiarz, V. W. Ballarotto and J. R. Reynolds, *ACS Applied Materials & Interfaces*, 2011, **3**, 1022-1032.
31. C. M. Amb, P. M. Beaujuge and J. R. Reynolds, *Advanced Materials*, 2010, **22**, 724-728.
32. J. Jensen and F. C. Krebs, *Advanced Materials*, 2014, **26**, 7231-7234.
33. M. Sendur, A. Balan, D. Baran, B. Karabay and L. Toppare, *Organic Electronics*, 2010, **11**, 1877-1885.
34. P. Shi, C. M. Amb, A. L. Dyer and J. R. Reynolds, *ACS Applied Materials & Interfaces*, 2012, **4**, 6512-6521.
35. M. İçli, M. Pamuk, F. Algi, A. M. Önal and A. Cihaner, *Chemistry of Materials*, 2010, **22**, 4034-4044.
36. W. T. Neo, L. M. Loo, J. Song, X. Wang, C. M. Cho, H. S. On Chan, Y. Zong and J. Xu, *Polymer Chemistry*, 2013, **4**, 4663-4675.
37. G. Hżalan, A. Balan, D. Baran and L. Toppare, *Journal of Materials Chemistry*, 2011, **21**, 1804-1809.
38. A. Balan, D. Baran and L. Toppare, *Polymer Chemistry*, 2011, **2**, 1029-1043.
39. A. Durmus, G. E. Gunbas and L. Toppare, *Chemistry of Materials*, 2007, **19**, 6247-6251.
40. F. Algi and A. Cihaner, *Organic Electronics*, 2009, **10**, 704-710.
41. H. Akpınar, A. Balan, D. Baran, E. K. Ünver and L. Toppare, *Polymer*, 2010, **51**, 6123-6131.
42. A. G. Nurioglu, H. Akpınar, M. Sendur and L. Toppare, *Journal of Polymer Science Part A: Polymer Chemistry*, 2012, **50**, 3499-3506.
43. Q. Ye, C. M. Cho, W. T. Neo, J. Xu, *SG Patent*, 10201404150Q, 2014.
44. R. G. Harvey, *Polycyclic Aromatic Hydrocarbons: Chemistry and Carcinogenicity*, Cambridge University Press, 1991.
45. R. Mondal, H. A. Becerril, E. Verploegen, D. Kim, J. E. Norton, S. Ko, N. Miyaki, S. Lee, M. F. Toney, J.-L. Bredas, M. D. McGehee and Z. Bao, *Journal of Materials Chemistry*, 2010, **20**, 5823-5834.
46. I. F. Perepichka, S. Roquet, P. Leriche, J.-M. Raimundo, P. Frère and J. Roncali, *Chemistry – A European Journal*, 2006, **12**, 2960-2966.
47. K.-S. Chen, Y. Zhang, H.-L. Yip, Y. Sun, J. A. Davies, C. Ting, C.-P. Chen and A. K. Y. Jen, *Organic Electronics*, 2011, **12**, 794-801.
48. J. Aragó, P. M. Viruela, E. Ortí, R. Malavé Osuna, B. Vercelli, G. Zotti, V. Hernández, J. T. López Navarrete, J. T. Henssler, A. J. Matzger, Y. Suzuki and S. Yamaguchi, *Chemistry – A European Journal*, 2010, **16**, 5481-5491.
49. M. L. Carl, M. Yan Ping, R. P. Agata and S. Francesca, *Electrical and Optical Properties of Electrochromic Devices Utilizing Polymer Electrodes*, 1990.
50. A. K. Agrawal and S. A. Jenekhe, *Chemistry of Materials*, 1996, **8**, 579-589.
51. C. L. Gaupp, D. M. Welsh, R. D. Rauh and J. R. Reynolds, *Chemistry of Materials*, 2002, **14**, 3964-3970.
52. J.-H. Huang, C.-Y. Hsu, C.-W. Hu, C.-W. Chu and K.-C. Ho, *ACS Applied Materials & Interfaces*, 2010, **2**, 351-359.
53. D. Aradilla, J. Casanovas, F. Estrany, J. I. Iribarren and C. Aleman, *Polymer Chemistry*, 2012, **3**, 436-449.
54. X. Guo, A. Facchetti and T. J. Marks, *Chemical Reviews*, 2014, **114**, 8943-9021.

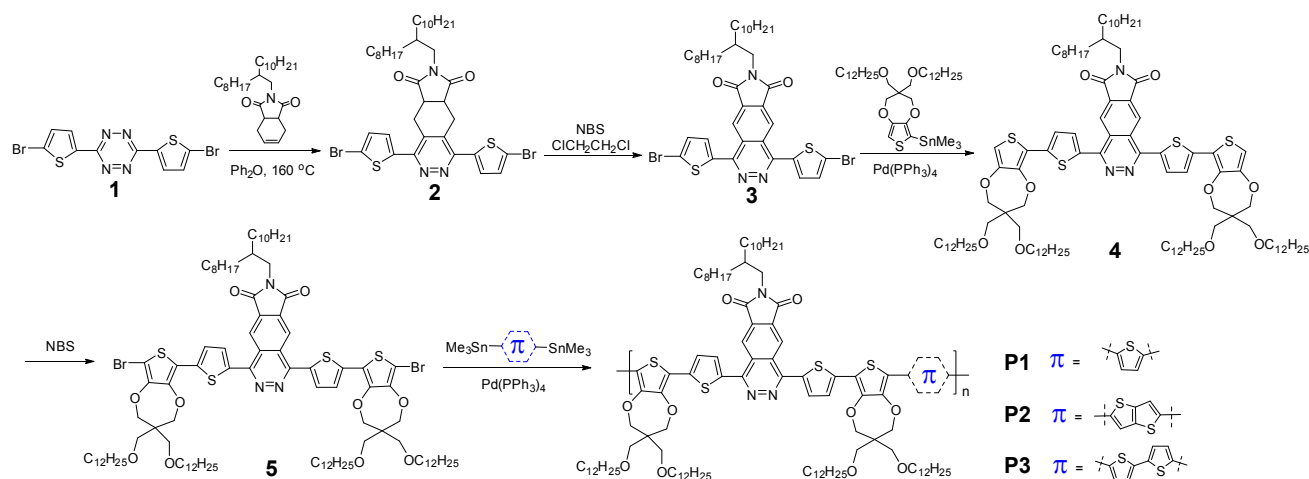
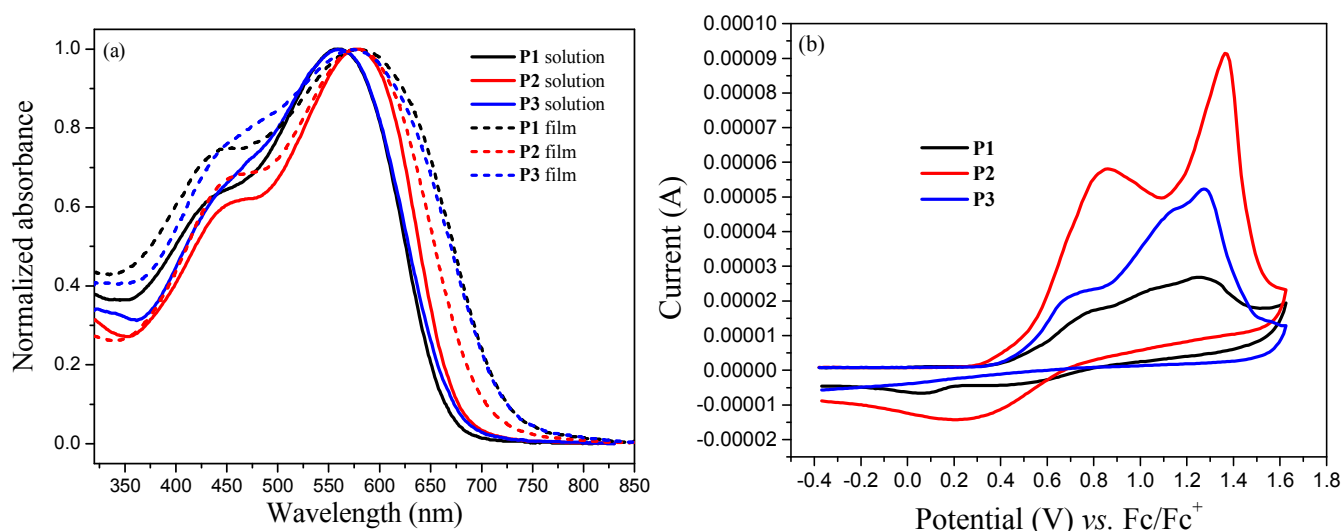
Scheme 1 Synthetic routes leading to **P1-P3**.

Fig. 1 (a) Normalized UV-vis absorption spectra of **P1-P3** in chlorobenzene and as thin films. (b) Cyclic voltammograms of **P1-P3** thin films in 0.1M $\text{LiClO}_4/\text{ACN}$ electrolyte/solvent couple at a scan rate of 50 mV/s calibrated vs. ferrocene/ferrocenium couple.

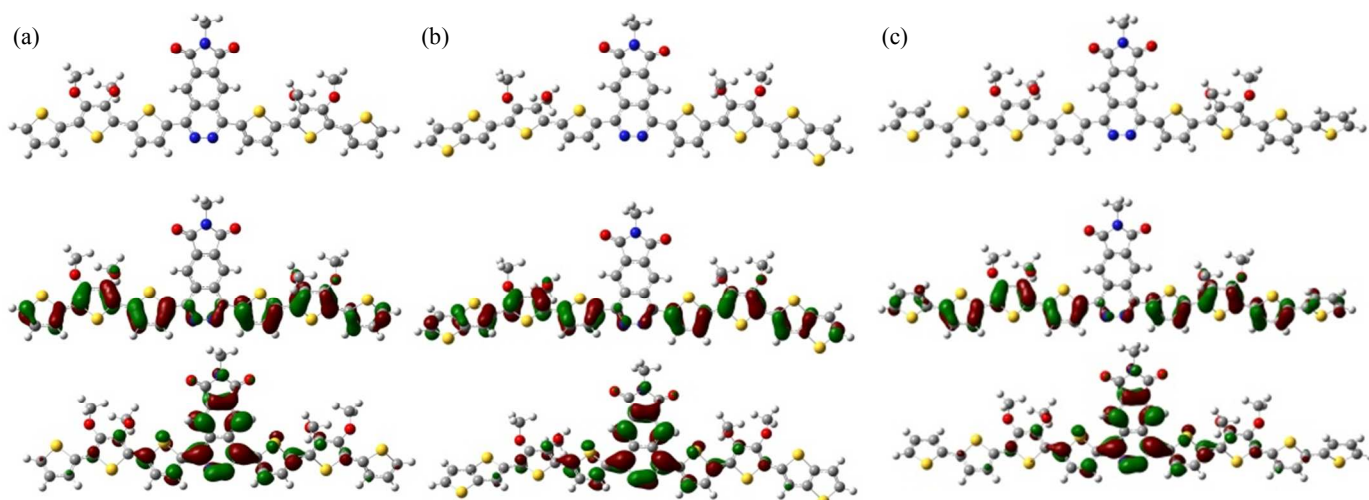


Fig. 2 Optimized geometries (top) and charge-density isosurfaces for the HOMO (middle) and LUMO (bottom) levels of (a) **M1**, (b) **M2** and (c) **M3** which are monomeric model compounds for **P1-P3** respectively.

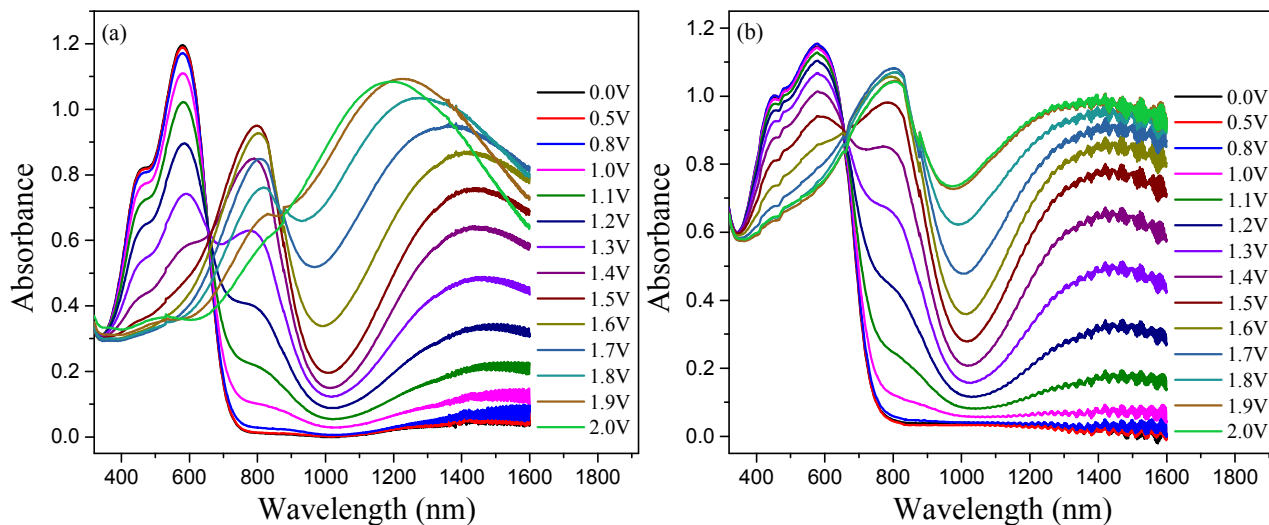


Fig. 3 Spectroelectrochemical graphs of (a) spin-coated (b) drop-cast **P2** devices at various applied potentials.

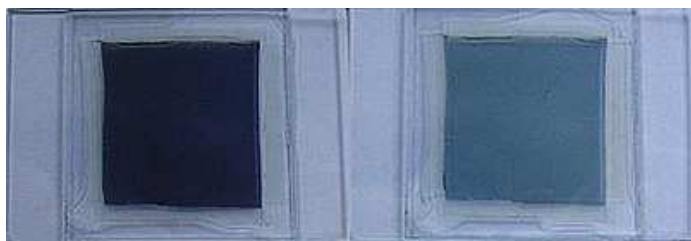


Fig. 4 Photos of **P2** spin-coated device in its neutral (left) and 2.0 V (right) states.

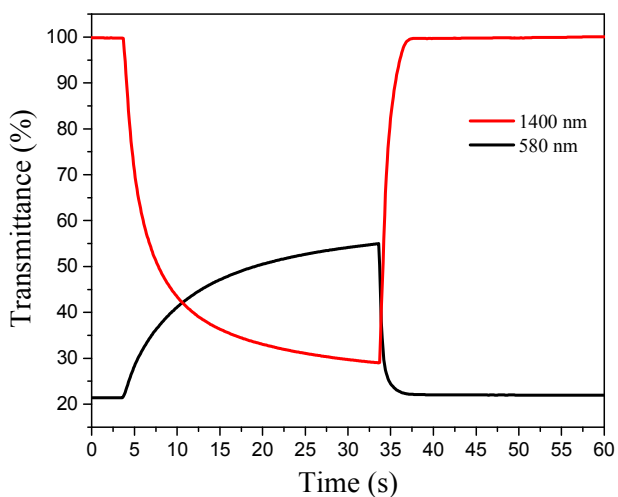


Fig. 5 Switching behaviour of **P2** device in the visible (λ_{max}) and NIR (1400 nm) regions between +1.6 and -1.6 V.

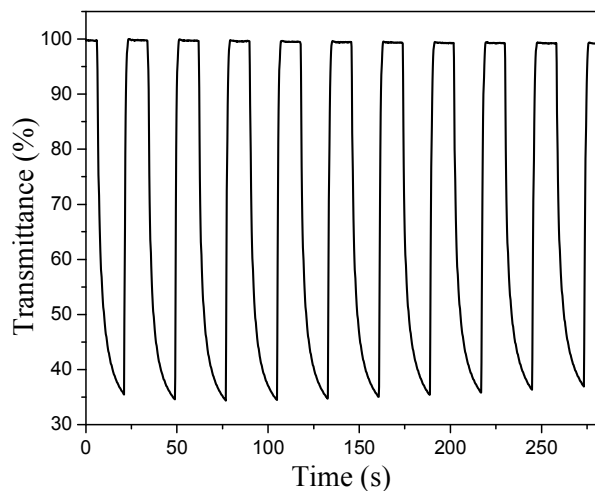


Fig. 6 Transmittance-time profile of **P2** device at 1400 nm between +1.6 and -1.6 V for 10 cycles.

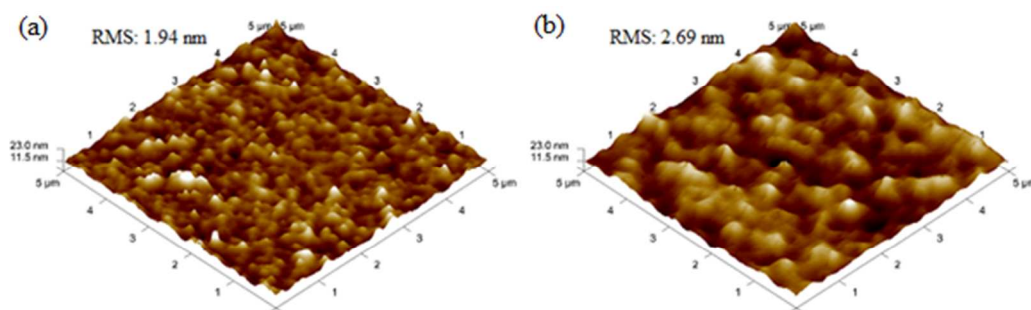


Fig. 7 AFM images of (a) spin-coated (b) drop-cast **P2** thin films. Scan size: 5×5 μm.

Table 1 Synthetic Yields, Molecular Weights, Polydispersity and Thermal Data of **P1-P3**

| Polymer | Yield (%) | M_n | M_w | Polydispersity | T_d (in N_2) (°C) |
|-----------|-----------|--------|--------|----------------|------------------------|
| P1 | 74 | 18,000 | 31,000 | 1.73 | 276 |
| P2 | 72 | 21,000 | 35,000 | 1.82 | 288 |
| P3 | 55 | 23,000 | 41,000 | 2.01 | 270 |

M_n : the number-average molecular weight. M_w : the weight-average molecular weight. T_d : the decomposition temperature at which 5% weight loss occurs.

Table 2 Summary of Optical and Electrochemical Properties of **P1-P3**

| | λ_{max} , solution (nm) | λ_{max} , film (nm) | λ_{onset} , film (nm) | $E_{g,opt}$ (eV) | HOMO (eV) | LUMO (eV)* |
|-----------|---------------------------------|-----------------------------|-------------------------------|------------------|-----------|------------|
| P1 | 559 | 576 | 722 | 1.72 | -5.27 | -3.55 |
| P2 | 577 | 577 | 698 | 1.78 | -5.29 | -3.51 |
| P3 | 559 | 574 | 719 | 1.72 | -5.28 | -3.56 |

*LUMO = HOMO – $E_{g,opt}$

Table 3 Summary of Electrochromic Performance of **P1-P3** ECDs

| | Optical contrast (%) | | Bleaching time (s) | | Coloration time (s) | | CE (cm ² /C) | |
|-----------|------------------------------|---------|------------------------------|---------|------------------------------|---------|------------------------------|---------|
| | λ_{max} (vis) | 1400 nm | λ_{max} (vis) | 1400 nm | λ_{max} (vis) | 1400 nm | λ_{max} (vis) | 1400 nm |
| P1 | 11 | 58 | 23.2 | 17.6 | 4.0 | 23.6 | 205 | 379 |
| P2 | 34 | 71 | 23.0 | 2.59 | 1.8 | 17.7 | 471 | 651 |
| P3 | 14 | 62 | 25.3 | 17.9 | 4.5 | 23.6 | 274 | 366 |